Advanced Robotics, Vol. 21, No. 1-2, pp. 65–85 (2007)

Also available online - www.brill.nl/ar

Full paper

Doping effects on robotic systems with ionic polymer–metal composite actuators

NORIHIRO KAMAMICHI [1,*], MASAKI YAMAKITA [1,2], TAKAHIRO KOZUKI [2], KINJI ASAKA [1,3] and ZHI-WEI LUO [1,4]

[1] *Bio-Mimetic Control Research Center, The Institute of Physical and Chemical Research (RIKEN), 2271-130 Anagahora, Shimoshidami, Moriyama-ku, Nagoya 463-0003, Japan*
[2] *Department of Mechanical and Control Engineering, Tokyo Institute of Technology, 2-12-1 Oh-okayama, Meguro-ku, Tokyo 152-8552, Japan*
[3] *Research Institute for Cell Engineering, National Institute of Advanced Industrial Science and Technology (AIST), 1-8-31 Midorigaoka, Ikeda, Osaka 563-8577, Japan*
[4] *Department of Computer and Systems Engineering, Faculty of Engineering, Kobe University, 1-1, Rokkodai, Nada-ku, Kobe 657-8501, Japan*

Received 14 October 2005; accepted 2 January 2006

Abstract—Ionic polymer–metal composite (IPMC) materials are one of the most promising electro-active polymer actuators for applications, and have good properties of response and durability. The characteristics of IPMC materials depend on the type of counter-ion. When applied to mechanical systems such as a robot, there exist possibilities to change the properties of the system dynamics by changing the counter-ions and system parameters according to the environment or purpose. We focus on this 'doping effect' property of the system and will verify the effect on robotic applications. In this paper, we consider dynamic walking of a small-sized biped robot and swimming motion of a snake-like robot, and demonstrate the doping effects by numerical simulations and experiments.

Keywords: Ionic polymer–metal composite actuator; electro-active polymer; robotic application; doping effect.

1. INTRODUCTION

High polymer gel actuators are one of the candidates for artificial muscle actuators due to their softness and miniaturizability. Electro-active polymers (EAPs) [1], which respond to electric stimuli with a shape change, have the potential capability of large displacement, quick response and operativity, and have received much attention from engineers and researchers in many disciplines, e.g., robotics, medical services, the toy industry, etc.

*To whom correspondence should be addressed. E-mail: nkama@bmc.riken.jp

Ionic polymer–metal composite (IPMC) [2], which is also known as ionic conducting polymer gel film (ICPF), is one of the most promising EAP actuators for applications, and has good properties of response and flexibility. IPMC actuators also have another noteworthy property — the characteristics of the bending motion are highly dependent on counter-ions [3]. When applied to mechanical systems such as a robot, there exist possibilities to change the properties of the system dynamics according to the environment or purpose. We call this property the 'doping effect' and will verify the effect on robotic applications.

If we consider walking applications, we might be able to change the property so that the actuator is suitable for slow walking with low energy consumption or fast walking with high energy consumption, or even running. For a small-sized autonomous robot, the energy supply and consumption are important problems. We might be able to transfer power through the use of an electromagnetic wave; however, in terms of usability and constraints from the environment, it is hoped that systems are self-contained. For the miniaturization of systems, the capacity of the battery is limited and energy efficiency should be high. Therefore, it is important for the actuator to be adjusted to the properties by doped counter-ions according to the purpose, since it is difficult to change the properties by changing driving voltages due to the limitation of the applied voltage.

In order to verify the doping effect, we consider walking control of a small-sized biped robot and propulsive control of a snake-like swimming robot. Based on numerical simulations and experiments, we investigate the validity of the adaptation with doping of the actuator.

2. IPMC ACTUATOR

IPMC is one of the most promising EAP actuators for applications, and is produced by chemically plating gold or platinum on a perfluorosulfonic acid membrane known as an ion-exchange membrane. When input voltage is applied to metal layers on both surface, it bends in high speed (Fig. 1). The characteristics of IPMC are as:

- Driving voltage is low (1–2 V).

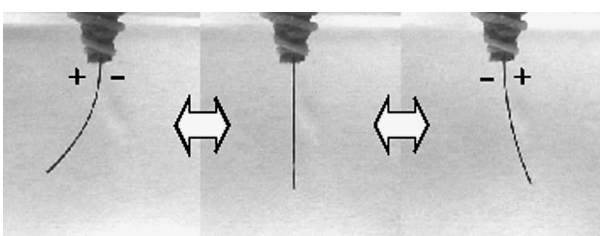

Figure 1. Bending behavior of the IPMC film.

- Speed of response is fast (above 100 Hz, the bandwidth is highly dependent of the thickness of the film).
- It is durable and chemically stable (it is possible to bend over 10^6 times).
- It is a flexible material.
- It moves in water and in wet conditions.
- Miniaturization and weight saving is possible.
- It is silent.
- It can be used as a sensor.

By exploiting these characteristics, IPMC actuators have been applied to robotic applications such as a fish-type robot [4–7], a snake-like robot [8], a wiper for a nanorover [9], a micromanipurator [10], a distributed actuation system [10], etc. In the following, another noteworthy property of IPMC is considered, i.e., changing the dynamic properties by changing the doped counter-ion.

2.1. Doping effect

It is known that IPMC changes its bending characteristics with respect to the doped counter-ions [3]. Figure 2 shows the responses of linear actuators, (see Section 3.2) for the same input voltage of 2.5 V, which are doped with sodium (Na^+), cesium (Cs^+) and tetraethylammonium (TEA^+) as the counter-ion, respectively. From Fig. 2, it is observed that the raising time of the actuator with Na^+ is shorter than with Cs^+ and the raising time of that with TEA^+ is the largest. On the other hand, the decay tendency of the response is large for the actuator with Na^+ or Cs^+, but it is very small for that with TEA^+. The doping of the counter-ion is easily done by just putting the actuator in a solution containing the target counter-ion and higher condensed counter-ions are doped into IPMC films. Also, the change of the doped ion is reversible. The property suggests that the characteristics of the actuator can be changed depending on the required purposes. Reference [3] described the doping effect of IPMC films, and reported the physical and chemical aspects of these property; however, it only considered the dynamics of IPMC film. Based on observations, we consider the doping effect on robotic applications, i.e., the change of the dynamics of robot's motion, which is caused by mutual interference between the dynamics of the robot and that of the actuator.

In Section 3, we will show the effect of the doping on walking pattern and efficiency of a small biped robot. In Section 4, we will show simulated and experimental results of the doping effect on swimming motion and efficiency on a snake-like robot.

3. APPLICATION TO A BIPED WALKING ROBOT

This section addresses an application of an IPMC actuator to a small-sized biped walking robot, and the realization and doping effect of walking are investigated

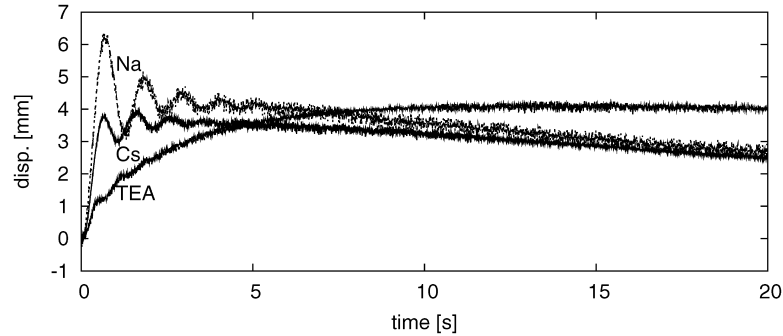

(a)

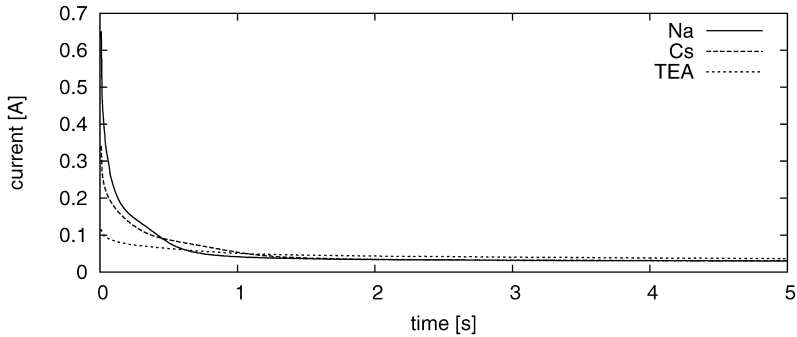

(b)

Figure 2. Response with various counter-ions. (a) Displacement. (b) Current.

by numerical simulations. For walking applications, we applied the IPMC linear actuators that were developed in a previous work [11].

3.1. Model of the biped walking robot

Figure 3 shows a model of the biped walking robot. Parameters of the robot are set as $m_\mathrm{l} = 0.005$ kg, $m_\mathrm{h} = 0.010$ kg, $a = 0.05$ m, $b = 0.05$ m, $l = 0.10$ m, $r = 0.004$ m and $g = 9.81$ m/s^2. This small biped robot can exhibit 'passive dynamic walking' [12] without any actuator on a gentle slope. In the following simulation, we assume that actuators are attached between legs as in the right-hand side of Fig. 3, that contact between a leg and the ground is pin contact, and that collision of the swing leg with the ground is perfectly inelastic.

3.2. IPMC linear actuator

The proposed linear actuator is composed of many basic units connected in parallel and serial so that enough force and displacement can be obtained. The structure of the elementary unit is shown in Fig. 4. This elementary unit consists of four IPMC films and one side of the unit is formed from a pair of films which are connected

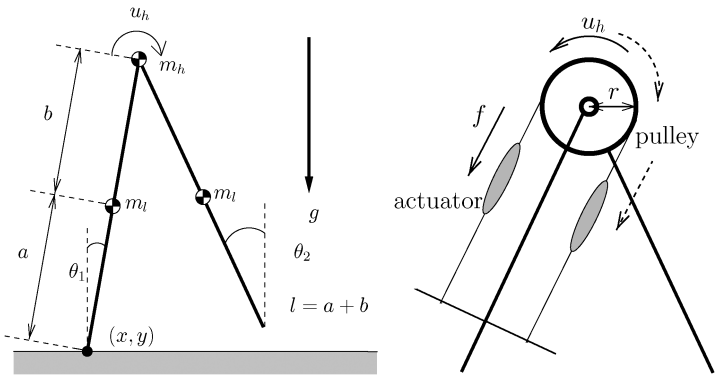

Figure 3. Model of the biped walking machine.

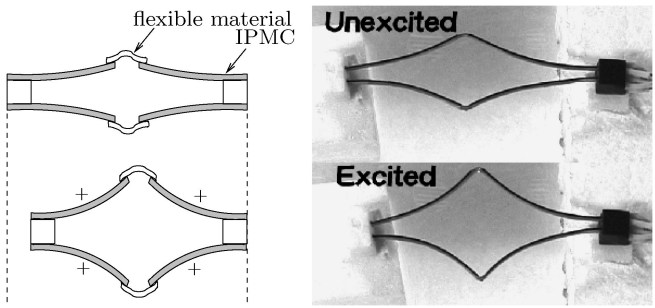

Figure 4. Structure of the IPMC linear actuator.

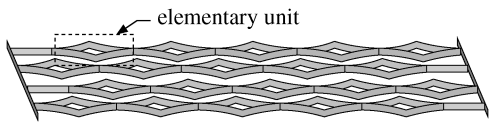

Figure 5. Basic concept of the IPMC linear actuator.

by a flexible material or the same thin film. When an input voltage is applied to electrodes of the surface with the anode outside, each membrane bends outside, i.e. the actuator is constricted. The actuation force and displacement of each unit are small; however, the elementary units are able to be connected in parallel and series as in Fig. 5, so that the actuator can realize the desired force and displacement. By shifting the series of elementary units by half pitch to avoid interference as in Fig. 5, the total actuator is made compact, and high power/volume and miniaturization are realized.

3.3. Walking simulations

IPMC actuators have been modeled in various ways as a black or gray box model [10, 13], and a detailed model in consideration of the physical and chemical phenomenon [14, 15]; however, it is difficult to represent these models by systems

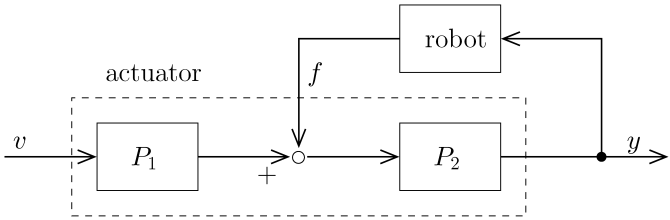

Figure 6. Block diagram of the simulator.

of ordinary differential equations because of their complexity. In this paper, a model of the actuator was identified from input–output data as a linear time invariant (LTI) system as shown in Fig. 6, where P_1 and P_2 are LTI systems. $P_1(s)$ represents the dynamics from an input voltage to a force generated by electric stimuli. $P_2(s)$ represents the dynamics from a force, which is exerted on the actuator, to a displacement of the actuator, where the force is assumed to be the difference between the generated force and external force from the robot. In the simulation, we constructed the models of the actuator and the robot, and these models were combined by the constraint condition of the position of the robot and the displacement of the actuator. Since the information about the actuator's acceleration is involved in the simulations, we identified the model of P_2 with an appropriate relative degree. See Ref. [11] for details. In this paper, we compare the motion of the robot with an IPMC actuator doped with several counter-ions. Each actuator model was identified from the experimental results.

Figure 7 shows the simulated results of walking on level ground. The number of units connected in parallel and series is set as 4 and 3, respectively. In this simulation, we applied a square pulse as an input voltage whose cycle is 0.48 s and whose amplitude is 2.5 V. From the results, it can be seen that the one-periodic walking gait is generated and the walking cycle synchronizes with the cycle of the input signal. We also carried out preliminary experiments on walking control (refer to Ref. [16]).

3.4. Doping effect on walking

As shown above, the bending characteristics of IPMC film are highly affected by the doped counter-ion. There exist possibilities to change the properties of the actuator according to the environment or purpose. If we consider the walking application, we can change the property so that the actuator is suitable for slow walking with low energy consumption or fast walking with high energy consumption, or even running. We investigate the possibility of adaptation with doping of the actuator for walking control by numerical simulations. Recall that the doped ion can be exchanged as many times as required.

We compare walking speeds and walking efficiencies for actuators which are composed of IPMC films doped with Na^+ and Cs^+ for the same input voltage. The

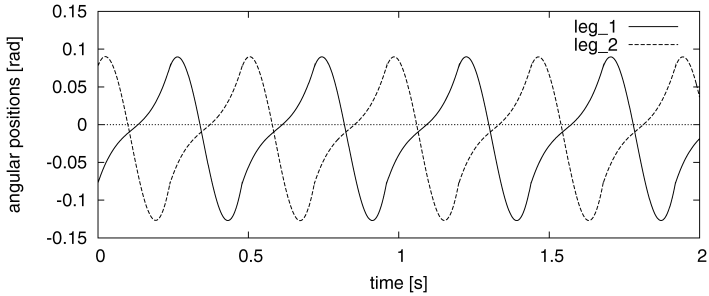

(a)

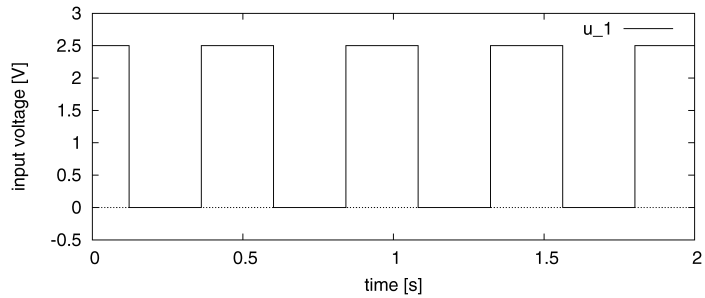

(b)

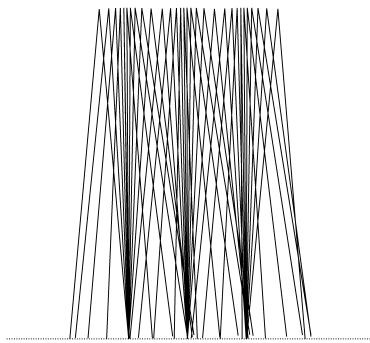

(c)

Figure 7. Simulated results of walking on level ground. (a) Angular positions. (b) Input. (c) Stick diagram.

input voltage is rectangular, its amplitude is 2.5 V and it is applied to the system in an open loop fashion.

Figure 8a shows a plot of the average walking speed with respect to the applied frequency of the input where the solid line shows the plot for the actuator with Na^+ and the dotted line for that with Cs^+. From Fig. 8 it can be seen that if the same control frequency input is applied for the robot, faster walking is realized by the actuator doped with Na^+ than by that with Cs^+. The maximum speed of the robot doped with Na^+ is higher than that doped with Cs^+. Note that this kind of property may not exist if the parameters of the robot are not properly designed. Thus, the

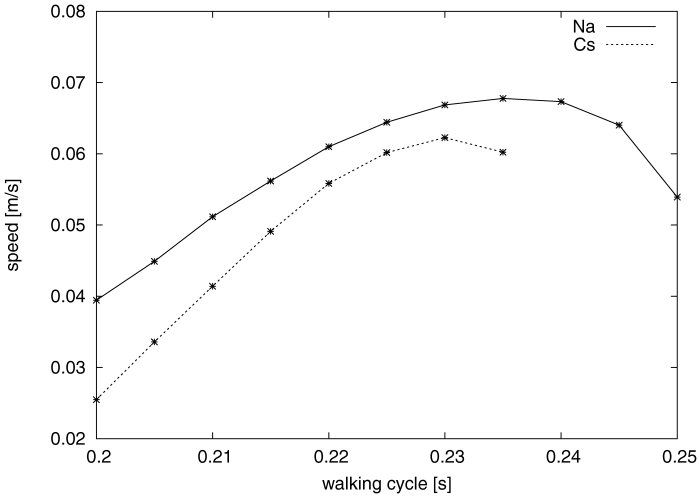

(a)

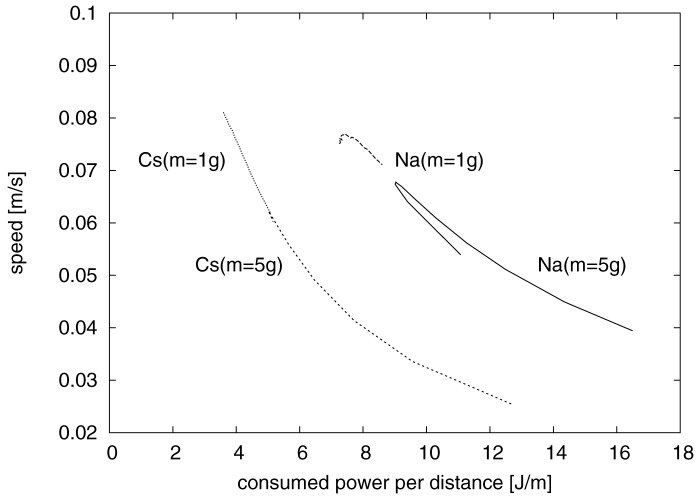

(b)

Figure 8. Simulated results of the doping effect. (a) Average speed *versus* walking cycle. (b) Average speed *versus* average input power.

design of the robot is important for the doping to be effective for adaptation of walking.

Figure 8b shows a plot of the walking speed with respect to the averaged consumed energy per distance. The average consumed energy per distance is equivalent to the locomotion performance (efficiency) and it was calculated as consumed power divided by the velocity of the movement. Since the input current for the actuator is almost irrelevant to the walking pattern, the peak value of the injected current of the actuator doped with Na^+ is large and the corresponding consumed power is large.

From the observation, it can be suggested that if the input voltage is the same, the actuator doped with Na^+ realizes high-speed walking with high energy consumption and the one doped with Cs^+ can generate a slow walking pattern with low energy consumption when the mass is rather heavy, i.e., $m = 5$ g. On the other hand, when $m = 1$ g, the actuator with Cs^+ can realize a wide range of walking speeds with low energy consumption. From these results, it can be concluded that if the parameters of the system are adequately selected, IPMC actuators with a quick response should be used for quick motions and *vice versa*.

If possible, we should verify the doping effect on biped walking experimentally, however, the walking system is statically unstable and it was thus difficult to perform the experiments. In the application to a snake-like swimming robot which is explain in the next section, we verify the doping effects by numerical simulation and experiments.

4. APPLICATION TO A SNAKE-LIKE ROBOT

In the previous section, it was shown that the efficiency of walking with different walking speed was confirmed by numerical simulations. In this section, the doping effect is checked by a snake-like robot swimming on the surface of water by numerical simulation and experiment. IPMC can be used in water without any means of waterproofing and can realize biomimetic motion; therefore, it seems to be valid to apply the actuator for an underwater mobile robot.

4.1. Snake-like robot

Figure 9 shows the experimental machine — a three-link snake-like swimming robot with IPMC actuators. The frames of the robot are made of styrene foam, and thin fins are attached to the bottom of the body frame; each of the frames is connected by an IPMC film. The total mass of the robot is 0.6 g and total length is 120 mm. The IPMC film which we used in this experiment is Nafion® 117 (DuPont) plated with gold, the thickness of this film is about 200 μm under wet conditions, and it was cut into a ribbon with a width of 2 mm and length of 20 mm.

Figure 10 shows a simple model of the robot; x_0 and y_0 are coordinates of the head position, and θ_1, θ_2 and θ_3 are the angles of each link. For modeling of the robot,

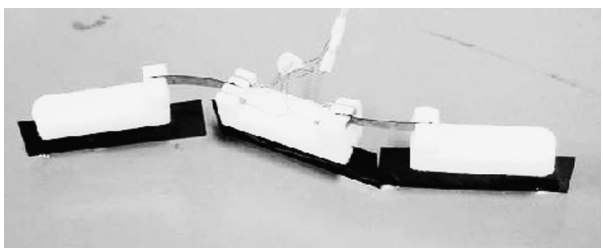

Figure 9. Snake-like robot using IPMC.

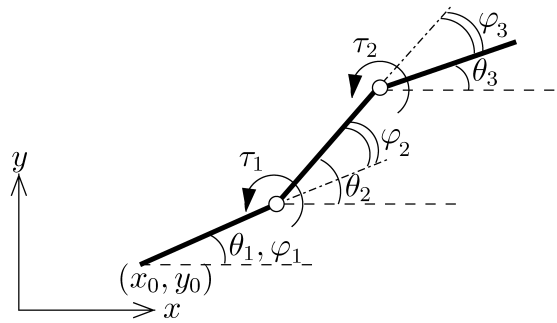

Figure 10. Model of the snake-like robot.

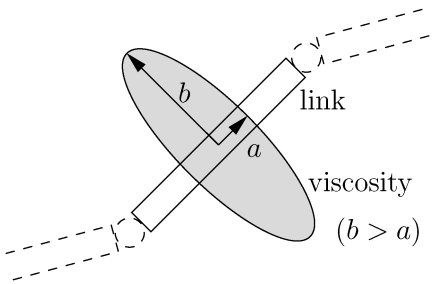

Figure 11. Model of viscosity.

refer to Ref. [17]. Due to the vertical fins at the bottom of the frames, the resistance of the water is small in the tangential direction of the body axis, while in the normal direction it is large. By bending the IPMC film of the joint with a phase shift, a propulsive force can be generated. In this paper, we consider the water resistance as viscous resistances and the coefficients of the viscosity are assumed to be distributed as an elliptical shape with respect to the directions shown in Fig. 11.

4.2. Numerical simulations

This section addresses numerical simulations of the snake-like robot with IPMC actuators, and demonstrates propulsion properties and doping effects. The methods of model identification and numerical simulation are similar to those of the walking simulation.

In this paper, we applied square pulses with a shifted phase as input voltages in an open-loop fashion. The parameters of the robot are set as values of an experimental machine and the coefficients of viscosity are identified from experimental results.

4.2.1. Propulsion property. Figure 12 shows the simulated results of propulsion. In this simulation, we applied a square pulse as input voltage whose cycle was 2 s, amplitude was 2.5 V and phase shift was 90°. The counter-ion of the actuator was Na^+. From the results, it can be seen that smooth propulsion is realized by applying appropriate phase-shifted inputs.

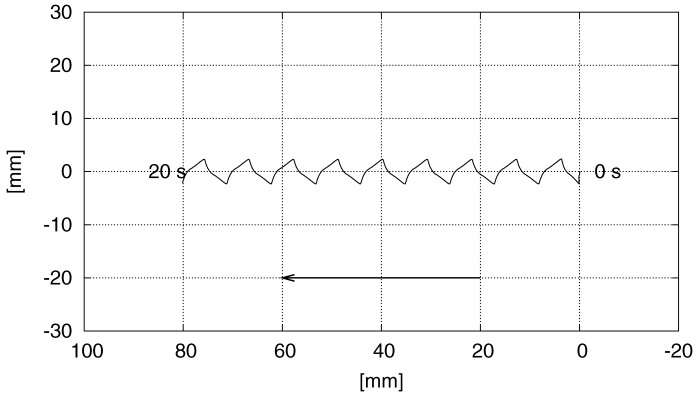

(a)

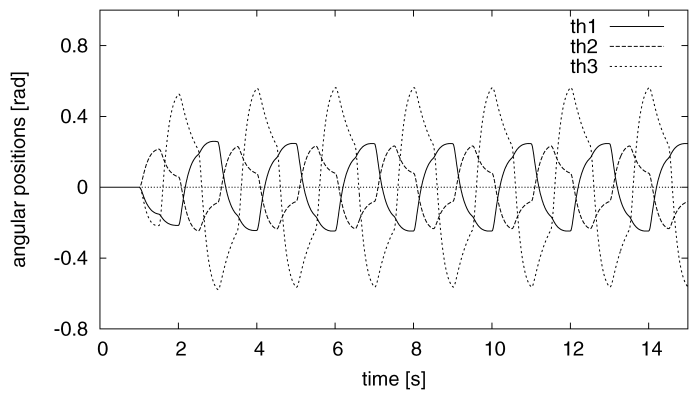

(b)

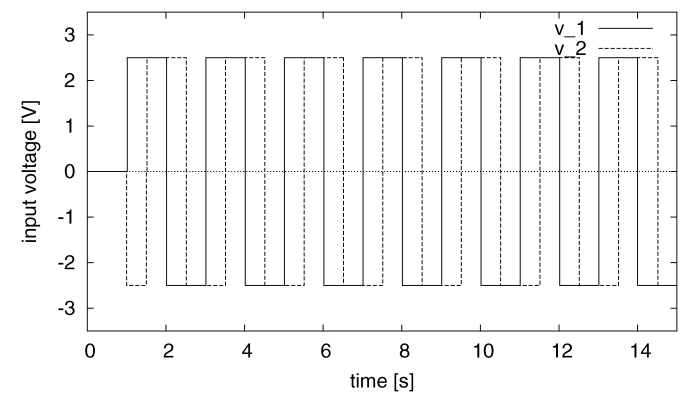

(c)

Figure 12. Simulated results of propulsive motion. (a) Trajectory of the head position. (b) Angular positions. (c) Input voltages.

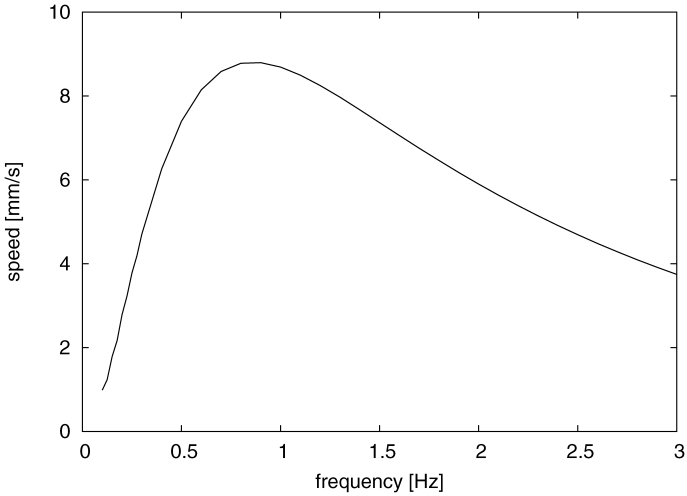

Figure 13. Simulated result (frequency *versus* average speed).

Figure 13 shows the simulated result of the relation between the input frequency and average speed over 10 and 20 s. We find that the propulsive speed greatly depends on the input frequency. When the input frequency is too high, the amplitude of bending motion becomes small and, therefore, an optimal frequency exists. The propulsion speed is also affected by the phase difference of the input voltage. Refer to the experimental results.

4.2.2. Doping effects. As shown in the walking simulations, we tested the 'doping effect' on the propulsive motion of snake-like robot by numerical simulations. We compared propulsive speed and efficiencies of the actuators doped with Na^+ and TEA^+ for the same input voltage. The input voltage is a square pulse whose amplitude is 2.5 V, and phase shift is 90°, and we simulated with various frequencies of the input.

Figure 14a shows the average propulsive speed with respect to the consumed power. It can be seen that faster propulsion is realized by the actuator doped with Na^+ rather than with TEA^+; however, the injected current of the actuator doped with Na^+ is large and the corresponding consumed power is large.

Figure 14b shows the average propulsive speed with respect to the consumed power per distance, which is equivalent to the efficiency of locomotion. A comparison with the same consumed power, if there is no power source limit, shows the actuator doped with Na^+ can move faster, and if we want to choose a more energy-efficient actuator, the actuator doped with TEA^+ should be selected since there is a domain of low consumed power only achieved by the actuator doped with TEA^+. There are many differences in the characteristics of the actuators doped with Na^+ and TEA^+ in terms of their speed and consumed power; however, it can be considered that the characteristics of the actuators can be adjusted for different purposes

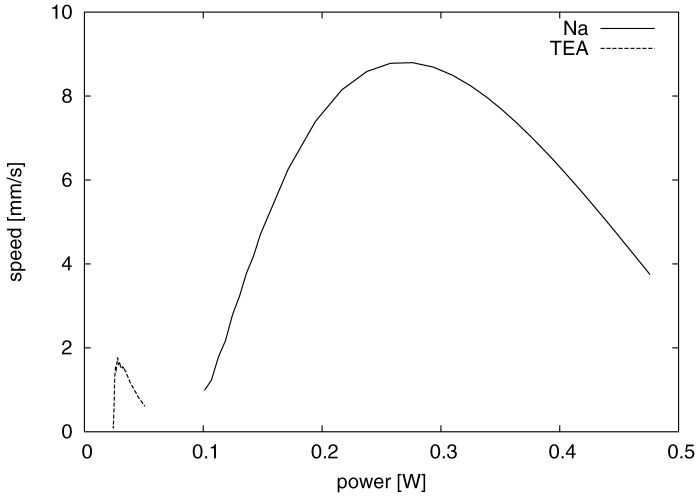

(a)

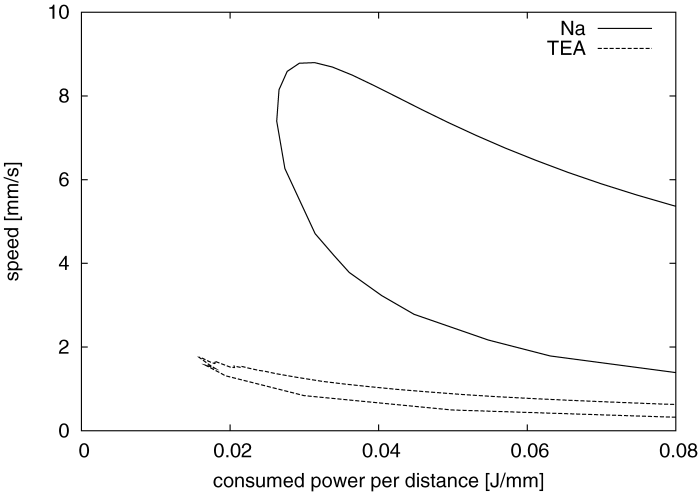

(b)

Figure 14. Simulated results of the doping effect. (a) Consumed power *versus* average speed. (b) Consumed energy per propulsive distance *versus* average speed.

by selecting an appropriate counter-ion or by mixing several ions in appropriate proportions.

4.3. Experiments

In order to check the performance of the robot and the doping effect, we also performed experiments using the snake-like robot shown in Fig. 9.

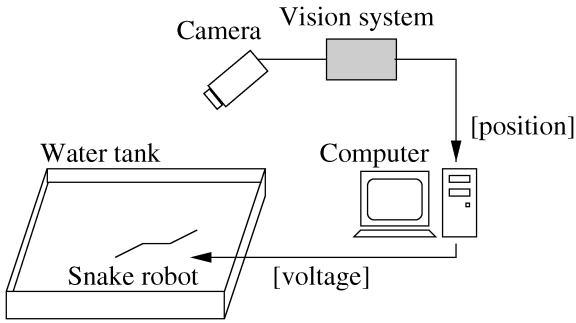

Figure 15. Experimental setup.

Figure 15 shows the experimental setup. The snake-like robot is located on the water surface of a water tank. Electric power is supplied externally by a wire. A vision system is used to measure the position of the robot.

4.3.1. Propulsion property. Figure 16 shows the experimental results with input signals whose cycle is 2 s, amplitude is 2.5 V, phase shift is 90° and the counter-ion is Na^+. From Fig. 16, it can be confirmed that the robot performed the undulating motion and moved forward. Figure 17 shows sequential photographs of the experiment.

Figure 18 shows the relation between the input frequency and average propulsive speed. The input voltages were square pulses of amplitude 2.5 V and phase shift 90°. The average speed is calculated from the moving distance over 10 and 20 s. The experiments were executed 3 times under each condition, and the data of each experiment and the mean values are plotted in Fig. 18. From Fig. 18, it can be seen that the propulsive speed changes greatly by changing the frequency of the input signal, similar to the simulated results. In the case of Na^+, the maximum speed was about 8 mm/s with an input signal of 0.5 Hz.

Figure 19 shows the relation between the phase shift of the input signals and the average propulsive speed. In the experiments, the inputs voltages were square pulses whose amplitude was 2.5 V and cycle was 1.6 s, and the counter-ion was Na^+. It is observed that the propulsive speed changes greatly by shifting the phases of the input signals and the direction of movement can be controlled. The curve of the propulsive speed of the experimental result is shifted a little in the negative direction under the influences of the wire and individual differences of IPMC films; however, the result is symmetrical with respect to the phase shift at 0°.

When comparing the simulation results with the experimental results, there exists some quantitative differences, e.g., the peak value of the speed or the shape of the property. In order to realize more accurate analysis, we might need to analyze the actual dynamics of the snake-like robot in consideration of the fluid dynamics and environment. However, it is considered that the simulation results were valid to represent the experimental motion because the results captured the property of motion qualitatively.

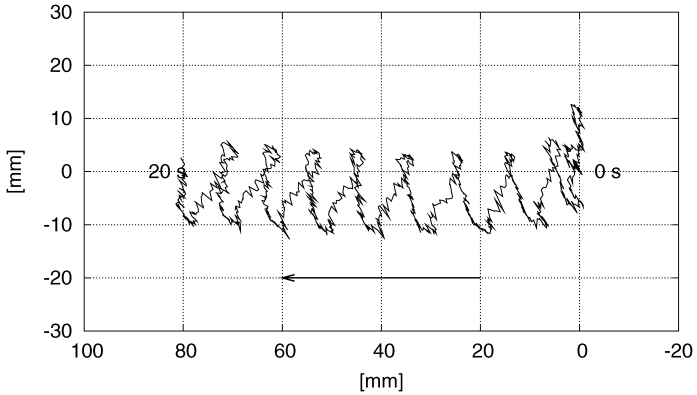

(a)

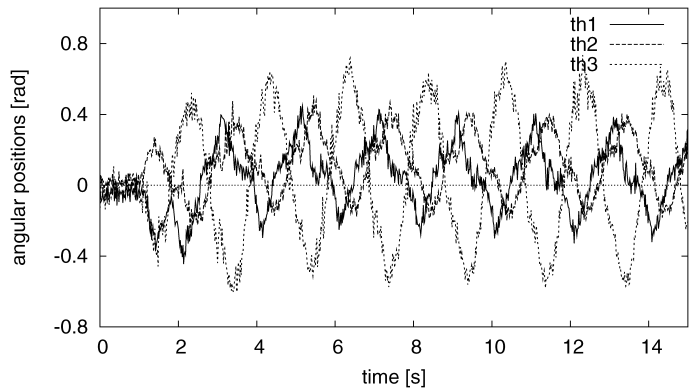

(b)

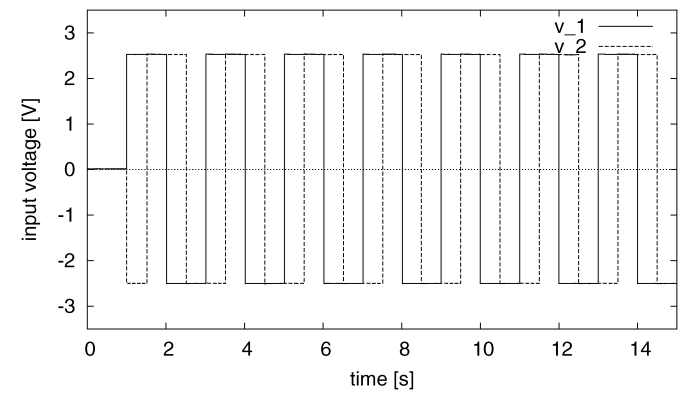

(c)

Figure 16. Experimental results. (a) Head position. (b) Angular positions. (c) Input voltages.

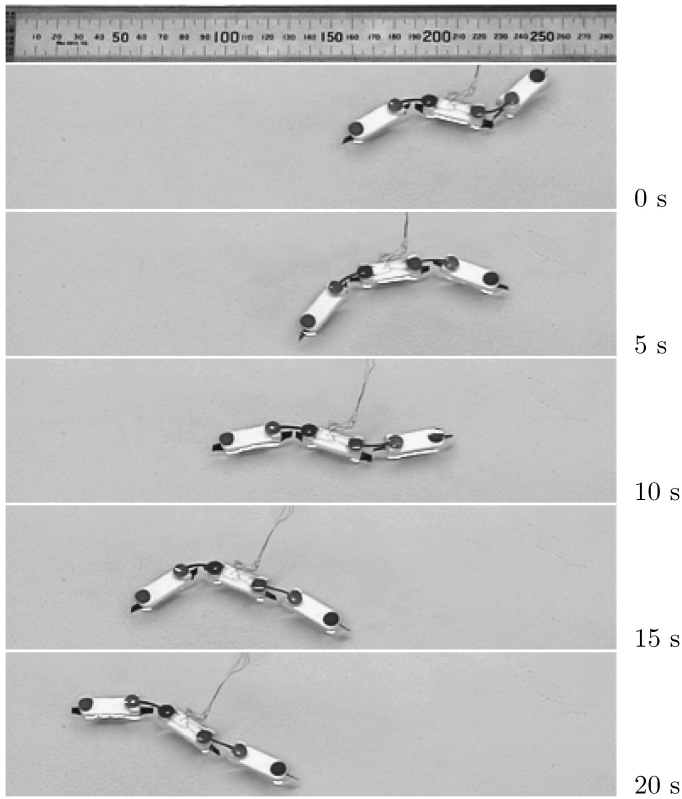

Figure 17. Sequential photographs of the experiment.

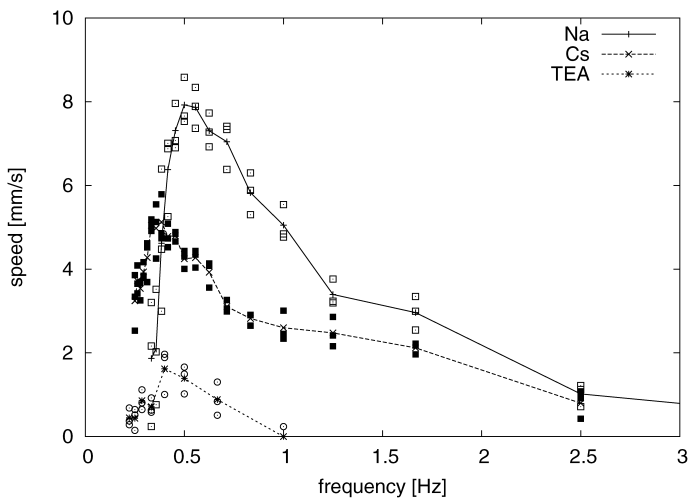

Figure 18. Experimental results (frequency *versus* average speed).

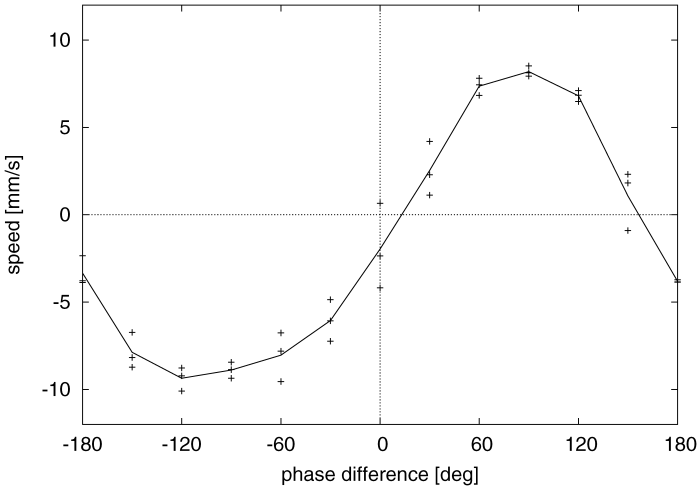

Figure 19. Experimental results (phase difference *versus* average speed).

4.3.2. Doping effect. In the application of the snake-like swimming robot, it also might be possible to change the property of the actuator so that the actuator is suitable for high-speed motion with high energy consumption or slow-speed motion with low energy consumption. In order to verify the doping effect, we performed experiments on IPMC actuators which were doped with Na^+, Cs^+ and TEA^+ as the counter-ion. Actuators were doped with each counter-ion by immersion in a solution of target counter-ions and experiments were carried out in tap water. We compared the propulsive speed and efficiencies of the actuators doped with each ion for the same input voltage. The inputs voltages were square pulses whose amplitude was 2.5 V and phase shift was 90°, and we repeated measurements with various input frequencies.

Figures 18 and 20 show the experimental results of the doping effect. Figure 18 shows the average propulsive speed with respect to the applied frequency of the input. It can be seen that the snake-like robot can move at a high speed in the order of Na^+, Cs^+ and TEA^+. In Fig. 20a, the average propulsive speed with respect to the consumed power is plotted. The snake-like robot doped with Na^+ can move faster; however, consumed power is large. If it need not move at high speed, we should use the actuators doped with other counter-ions which can be driven by low power. Figure 20b shows the average propulsion speed with respect to the consumed power per distance, which is equivalent to the efficiency of locomotion. If there is no limit to the capacity of the power source, it can be considered that the actuator doped with Na^+ is effective, since the robot can move in a short time; however, there is a region of low consumed power achieved only by the robot doped with TEA^+.

From the observation, it can be summarized that if the input voltage is the same, the actuator doped with Na^+ realizes high-speed swimming motion with high energy consumption, the actuator doped with TEA^+ can generate a slow swimming speed with a low energy consumption, and the actuator doped with Cs^+ has the

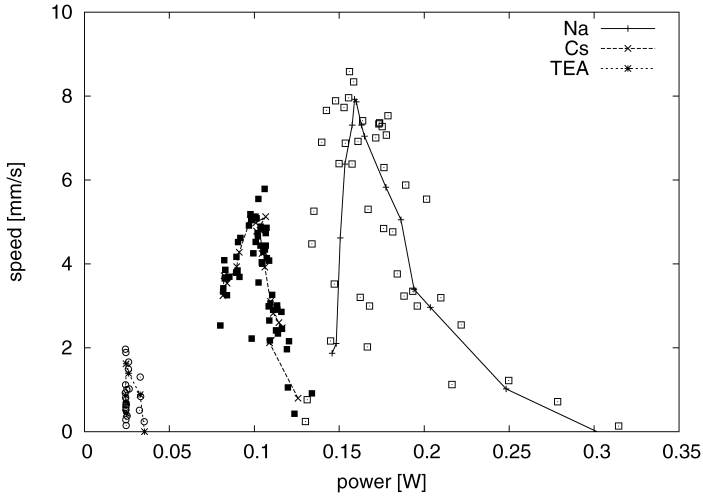

(a)

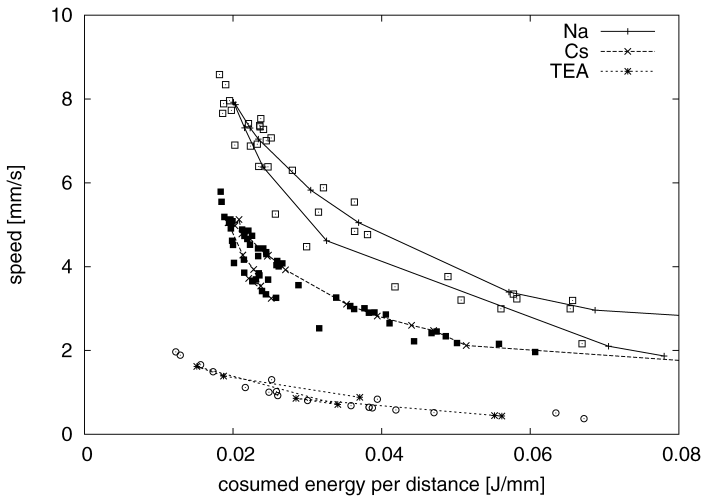

(b)

Figure 20. Experimental results of the doping effect. (a) Consumed power *versus* average speed. (b) Consumed energy per distance *versus* average speed.

intermediate characteristics of Na^+ and TEA^+, i.e., findings which are qualitatively consistent with the numerical simulations in the previous section. Note that the actuators are able to be adjusted to various characteristics for different purposes by selecting an appropriate counter-ion or by mixing several ions in appropriate proportions.

If we consider that the actuator doped with Na^+ was used under lower voltage so that the speed is the same as the one doped with TEA^+, the properties of energy consumption get close in this case of a snake-like swimming robot. It is, however, highly mutually concerned with the dynamics of the robot and that of

IPMC actuator. From the results of two application, i.e., the biped walking robot and the snake-like robot, the doping effect on robotic application is caused by the interference between the dynamics of the robot and that of the IPMC actuator. Actually, the characteristics and efficiency of the motion are affected by both the dynamics of the IPMC actuator and the robot. Therefore, we need to choose adequate physical parameters of the robot and the actuator. In this paper, we have shown the results under appropriate operating conditions for the response and the limitation of electrolysis. IPMC properties are usually non-linear; therefore, if we consider a larger input voltage or larger deformation, other analyses or discussions will be needed to take account of the nonlinearity.

5. CONCLUSIONS

We have discussed the doping effect of IPMC actuators, and its effects on a biped walking robot and a snake-like robot. It was shown by numerical simulations of walking control and by numerical simulation and experiment of swimming control of a snake-like robot that the properties of the actuator can be adjusted according to particular motions, i.e., slow-speed motion with low energy consumption or high-speed motion with high energy consumption. The doping effect on the robotic application greatly affects the dynamics of both the robot and IPMC actuator, so it is very effective for efficient robotic motions if the parameters of the dynamics of the robots are selected adequately. Systematic parameter design of robotic systems in which the doping effect is efficient is a future problem.

In order to apply the artificial muscle actuator to a general robotic system, there exist many problems such as limitation of output force; however, we believe the mutual evolution of improvements of actuator technology and the design of the control system is important for further applications.

REFERENCES

1. Y. Bar-Cohen, *Electroactive Polymer (EAP) Actuators as Artificial Muscles: Reality, Potential, and Challenges*. SPIE Press, Bellingham, WA (2001).
2. K. Oguro, K. Y. Kawami and H. Takenaka, Bending of an ion-conducting polymer film-electrode composite by an electric stimulus at low voltage, *J. Micromachine Soc.* **5**, 27–30 (1992) (in Japanese).
3. K. Onishi, S. Sewa, K. Asaka, N. Fujiwara and K. Oguro, The effects of counter ions on characterization and performance of a solid polymer electrolyte actuator, *Electrochim. Acta* **46**, 1233–1241 (2001).
4. M. Mojarrad and M. Shahinpoor, Biomimetic robotic propulsion using polymeric artificial muscles, in: *Proc. IEEE Int. Conf. on Robotics and Automation*, Albuquerque, NM, pp. 2152–2157 (1997).
5. S. Guo, T. Fukuda and K. Asaka, A new type of fish-like underwater microrobot, *IEEE/ASME Trans. Mechatron.* **8**, 136–141 (2003).
6. EAMEX Corp., http://www.eamex.co.jp.

7. J. Jung, B. Kim, Y. Tak and J.-O. Park, Undulatory tadpole robot (TadRob) using ionic polymer metal composite (IPMC) actuator, in: *Proc. IEEE/RSJ Int. Conf. on Intelligent Robots and Systems*, Las Vegas, NV, pp. 2133–2138 (2003).
8. Y. Nakabo, T. Mukai, K. Ogawa, N. Ohnishi and K. Asaka, Biomimetic soft robot using artificial muscle, in tutorial: *Electro-Active Polymer for Use in Robotics, IEEE/RSJ Int. Conf. on Intelligent Robots and Systems*, Sendai (2004).
9. Y. Bar-Cohen, S. P. Leary, A. Yavronian, K. Oguro, S. Tadokoro, J. Harrison, J. Smith and J. Su, Challenges to the application of IPMC as actuators of planetary mechanisms, in: *Proc. SPIE Int. Symp. on Smart Structures and Materials, EAPAD*, Newport Beach, CA, vol. **3987**, pp. 140–146 (2000).
10. S. Tadokoro, M. Konyo and K. Oguro, Modeling IPMC for design of actuation mechanisms, in: *Electroactive Polymer (EAP) Actuators as Artificial Muscles, Reality, Potential, and Challenges*, Y. Bar-Cohen (Ed.), pp. 331–366. SPIE Press, Bellingham, WA (2001).
11. M. Yamakita, N. Kamamichi, Y. Kaneda, K. Asaka and Z.-W. Luo, Development of an artificial muscle linear actuator using ionic polymer-metal composites, *Adv. Robotics* **18**, 383–399 (2004).
12. T. McGeer, Passive dynamic walking, *Int. J. Robotics Res.*, **9**, 62–82 (1990).
13. K. Mallavarapu, K. M. Newbury and D. J. Leo, Feedback control of the bending response of ionic polymer–metal composite actuators, in: *Proc. SPIE Int. Symp. on Smart Structures and Materials, EAPAD*, Newport Beach, CA, vol. 4329, pp. 301–310 (2001).
14. K. Asaka and K. Oguro, Bending of polyelectrolyte membrane platinum composites by electric stimuli Part II. Response kinetics, *J. Electroanal. Chem.* **480**, 186–198 (2000).
15. S. Tadokoro, M. Fukuhara, Y. Maeba, M. Konyo, T. Takamori and K. Oguro, A dynamical model of ICPF actuator considering ion-induced lateral strain for molluskan robotics, in: *Proc. IEEE Int. Conf. on Robotics and Automation*, Washington, DC, pp. 2010–2017 (2002).
16. M. Yamakita, N. Kamamichi, T. Kozuki, K. Asaka and Z.-W. Luo, Control of biped walking robot with IPMC linear actuator, in: *Proc. IEEE/ASME Int. Conf. on Advanced Intelligent Mechatronics*, Monterey, CA, pp. 48–53 (2005).
17. P. Prautsch and T. Mita, Control and analysis of the gait of snake robots, in: *Proc. IEEE Int. Conf. on Control Applications*, Hawaii, HI, pp. 502–507 (1999).

ABOUT THE AUTHORS

Norihiro Kamamichi received the BE, ME and DE degrees from Tokyo Institute of Technology in 2001, 2003 and 2006, respectively. He is currently a researcher at Bio-mimetic Control Research Center, RIKEN. His research interests include robotics, biped walking and soft actuators. He is a member of the RSJ, SICE and IEEE.

Masaki Yamakita received the BE, ME and DE degresees from Tokyo Institute of Technology in 1984, 1986 and 1989, respectively. From 1989 he was a research associate in the Department of Control Engineering, Tokyo Institute of Technology and from 1993 he was a Lectures at Toyohashi University of Technology. He is currently an Associate Professor in the Department of Mechanical and Control Engineering, Tokyo Institute of Technology. His research interests include robotics, learning control, robust and nonlinear control. He is a member of the IEEE, SICE, RSJ, etc.

Takahiro Kozuki received the BE and ME degrees from Tokyo Institute of Technology in 2004 and 2006, respectively. He studied robotics and control of legged robots in master's course student.

Kinji Asaka received the PhD degree in Science from Kyoto University in 1991. He is currently a Group Leader of the Artificial Cell Research Group, Research Institute for Cell Engineering, National Institute of Advanced Industrial Science and Technology. His current research interests include interfacial electrochemistry and polymer actuators. He is a member of the Society of Polymer Science, Japan and SICE.

Zhi-Wei Luo received the BS degree in Engineering from Huazhong University of Science and Technology, China in 1984, and the MS and DE degrees in Information Engineering in 1991 and 1992 from Nagoya University, Japan. From 1984 to 1986, he was a teacher at Suzhou University, China. From 1986 to 1988, he was a Visiting Scholar at Aichi Institute of Technology, Japan. From 1992 to 1994, he was an Assistant Professor of Toyohashi University of Technology, Japan. From 1994 to 1998, he was a Frontier Researcher at the Bio-mimetic Control Research Center, RIKEN. From 1999 to 2001, he was an Associate Professor of Yamagata University. He is currently a Laboratory Head of the Environment Adaptive Robotic Systems Laboratory, Bio-mimetic Control Research Center, RIKEN and Professor in the Department of Computer and Systems Engineering, Faculty of Engineering, Kobe University. His research interests include robotics, system control theory and bio-mimetics. He is a member of the RSJ, SICE and IEEE.